BULLETIN OF THE EARTHQUAKE
RESEARCH INSTITUTE
Vol. 54 (1979), pp. 1-29

# 1. *The Piezomagnetic Field Associated with the Mogi Model.*

By Yoichi SASAI,

Earthquake Research Institute.

(Received May 21, 1979)

## Summary

An analytical solution can be obtained for the piezomagnetic field accompanying a strain nucleus of the center of dilatation within the semi-infinite elastic medium. In volcanology, the problem is called the Mogi model, which successfully explains surface displacements around a volcano associated with its eruptions. The stress-induced magnetization within a uniformly magnetized crustal layer can be expressed in the form of a linear combination of stress components. The convolution integrals representing the piezomagnetic field are then evaluated by the Fourier transform method. The solution consists of combination of dipoles and quadrupoles at depth. Especially under appropriate conditions of actual volcanoes, the piezomagnetic field accompanying the Mogi model is equivalent to that of a magnetic dipole embedded at the dilating center. The stress-induced magnetization might be responsible for at least a portion of the rapid geomagnetic changes associated with eruptions of the Oshima volcano, Japan, although the dominant long-period variations would be of thermal origin.

## Introduction

A simple mechanical model was introduced by MOGI (1958) to interpret crustal deformations before and after volcanic eruptions. He adopted a hydrostatically pumped sphere as a model of the magma reservoir beneath the volcanic body. According to the elasticity theory, the surface displacements accompanying Mogi's model are equivalent to those of an idealized strain nucleus, namely a center of dilatation in the semi-infinite elastic medium. The problem had already been solved by YAMAKAWA (1955), whose results were employed by MOGI (1958). Observable surface deformations were successfully explained in some cases with a hydrostatic pressure amounting to a few kilobars or more (MOGI 1958, FISKE and KINOSHITA 1969). Another force source of magmatic intrusion type was proposed by YOKOYAMA (1971) so as to attain ground deformations more effectively. The distribution of normal stress across the surface of the source sphere can be represented by $P_0$ of the spherical harmonics in the case of the Mogi

model, while that of the Yokoyama model is a $P_1^1(\cos\theta)$ type. As far as ordinary values of mechanical strength are assumed for competent rocks within volcanoes, a fairly large amount of pressure changes are necessary even in the case of the Yokoyama model to interpret observed surface displacements. A stress-induced magnetic change is therefore anticipated, accompanying the volcanic activities.

The piezomagnetic effect of magnetized rocks has been well established during the past decades (NAGATA 1970, STACEY and BANERJEE 1974). The basic concept of the stress-induced volcano-magnetic effect was first proposed by STACEY, BARR and ROBSON (1965), who calculated the piezomagnetic anomaly field due to some particular stress distribution around a magma chamber. Their model calculation seems, however, to be somewhat inappropriate, because the stress field solution in the *infinite* elastic medium was adopted in their work. YUKUTAKE and TACHINAKA (1967) obtained the piezomagnetic field associated with a dilating cylinder at a depth parallel to the surface, in which boundary conditions at the surface are properly taken into account. Yukutake's model is nothing but a two-dimensional version of the Mogi model, which might be usefull in case of the fissure eruption. The piezomagnetic change accompanying the Mogi model itself was calculated by DAVIS (1976). All these model calculations were numerical ones, with elaborate computer work.

An analytical solution is presented here of the piezomagnetic field produced by the Mogi model. The situation is limited to the case of a point force source in the semi-infinite elastic medium with uniform magnetization from surface to a depth of Currie point isotherm. Only the reversible change with respect to the applied stress is considered here (See NAGATA 1970). The method is based on Fourier transforms of the convolution integrals. Direct suggestions were given to the present work by HAGIWARA (1977), who derived gravity change associated with the Mogi model by means of Fourier integral transforms.

The final result will be shown to have a very simple form. It is not intended in this paper to apply the present result to actual field data. A qualitative comparison will be made in the last section between two possible causes of the volcano-magnetic effect, namely (a) stress effect and (b) temperature effect.

## The Stress Field of the Mogi Model

We take the Cartesian and cylindrical coordinate systems as shown in Fig. 1, where a semi-infinite elastic body occupies $z \geqq 0$. The problem is to determine the stress field at an arbitrary point in the semi-infinite elastic medium when a small sphere at $(0, 0, D)$ suffers hydro-

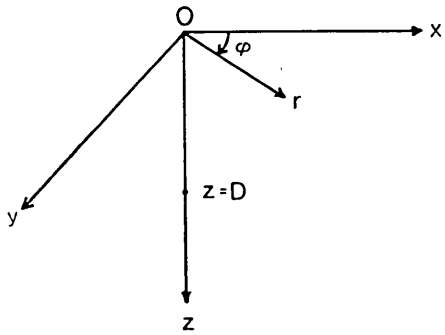


Fig. 1. Coordinates systems.

static pressure $\Delta P$ from inside. The displacement field of the present problem was obtained in a rather classical manner by ANDERSON (1936) and independently by YAMAKAWA (1955), whose solution might be available to derive the stress field by differentiation. We deal with the problem here in terms of the Love's strain function $\Phi$, which satisfies the following equation when there is no body force,

$$\nabla^2\nabla^2\Phi=0 \tag{1}$$

$$\left.\begin{aligned}\nabla^2&=\frac{\partial^2}{\partial x^2}+\frac{\partial^2}{\partial y^2}+\frac{\partial^2}{\partial z^2}\\&=\frac{\partial^2}{\partial r^2}+\frac{1}{r}\frac{\partial}{\partial r}+\frac{1}{r^2}\frac{\partial^2}{\partial\varphi^2}+\frac{\partial^2}{\partial z^2}\end{aligned}\right\} \tag{2}$$

The displacements are given by

$$2\mu u_r=-\frac{\partial^2\Phi}{\partial r\partial z}\,,\quad 2\mu u_\varphi=-\frac{1}{r}\frac{\partial^2\Phi}{\partial\varphi\partial z}\,,\quad 2\mu u_z=\left[2(1-\nu)\nabla^2-\frac{\partial^2}{\partial z^2}\right]\Phi \tag{3}$$

Six components of the stress tensor in the cylindrical coordinates are derived from the following formulae;

$$\left.\begin{aligned}\sigma_{rr}&=\frac{\partial}{\partial z}\left(\nu\nabla^2-\frac{\partial^2}{\partial r^2}\right)\Phi\\\sigma_{\varphi\varphi}&=\frac{\partial}{\partial z}\left(\nu\nabla^2-\frac{1}{r}\frac{\partial}{\partial r}-\frac{1}{r^2}\frac{\partial^2}{\partial\varphi^2}\right)\Phi\\\sigma_{zz}&=\frac{\partial}{\partial z}\left[(2-\nu)\nabla^2-\frac{\partial^2}{\partial z^2}\right]\Phi\\\sigma_{r\varphi}&=-\frac{\partial^3}{\partial r\partial\varphi\partial z}\left(\frac{\Phi}{r}\right)\\\sigma_{\varphi z}&=\frac{1}{r}\frac{\partial}{\partial\varphi}\left[(1-\nu)\nabla^2-\frac{\partial^2}{\partial z^2}\right]\Phi\\\sigma_{zr}&=\frac{\partial}{\partial r}\left[(1-\nu)\nabla^2-\frac{\partial^2}{\partial z^2}\right]\Phi\end{aligned}\right\} \tag{4}$$

$$\nu=\frac{\lambda}{2(\lambda+\mu)}$$

where $\nu$, $\lambda$ and $\mu$ are Poisson's ratio and Lame's constants.

MINDLIN and CHENG (1950) obtained expressions for various types of strain nuclei in the semi-infinite solid in terms of the Galerkin vector stress function. The strain function for a center of dilatation placed at a point $(0, 0, D)$ in the semi-infinite medium is given as follows (MINDLIN and CHENG 1950, See also HAGIWARA 1977);

$$\Phi=C\left\{\log(D-z+R_1)+\frac{\lambda-\mu}{\lambda+\mu}\log(z+D+R_2)-\frac{2z}{R_2}\right\} \tag{5}$$

where

$$\left.\begin{aligned} R_1&=\sqrt{r^2+(D-z)^2}\\ R_2&=\sqrt{r^2+(D+z)^2}\\ r&=\sqrt{x^2+y^2}\end{aligned}\right\} \tag{6}$$

The first term corresponds to a strain nucleus at $(0, 0, D)$ in the infinite medium, while the remainder is the sum of an image nucleus at $(0, 0, -D)$, and the solution of Boussinesq problem for the resultant normal load. The image nucleus cancels the tangential shear stress, and the Boussinesq solution nullifies the normal stress at the surface, respectively. The traction free boundary conditions at the surface are thus satisfied in the solution (5).

The coefficient $C$ should be determined elsewhere, which indicates the intensity of the strain nucleus having a dimension of the moment of force. Consider a small sphere of radius $a$ with its center at $(0, 0, D)$. Taking the spherical coordinates $(R, \theta, \varphi)$ centered at $(0, 0, D)$, the stress components in the spherical coordinates $\sigma_{RR}$, $\sigma_{\theta\theta}$, $\sigma_{R\theta}$ are related to those in the cylindrical ones $\sigma_{rr}$, $\sigma_{zz}$, $\sigma_{zr}$ as follows;

$$\left.\begin{aligned} \sigma_{RR}&=\frac{1}{R_1^2}\{\sigma_{rr}r^2+\sigma_{zz}(z-D)^2+2\sigma_{zr}r(z-D)\}\\ \sigma_{\theta\theta}&=\frac{1}{R_1^2}\{\sigma_{rr}(z-D)^2+\sigma_{zz}r^2-2\sigma_{zr}r(z-D)\}\\ \sigma_{R\theta}&=\frac{1}{R_1^2}\{(\sigma_r-\sigma_z)r(z-D)+\sigma_{zr}[(z-D)^2-r^2]\}\end{aligned}\right\} \tag{7}$$

Under the assumption that $a$ is small, i.e., $a\ll D$, so that $R_1\ll R_2$, the main contribution to the stress field is that of the first term, $\Phi_1=C\log(D-z+R_1)$. Substituting $\Phi_1$ into equations (4), we have stress components near the small sphere;

$$\left.\begin{aligned}\sigma_{rr}&=-C\frac{R_1^2-3r^2}{R_1^5}\\ \sigma_{zz}&=-C\frac{R_1^2-3(z-D)^2}{R_1^5}\\ \sigma_{zr}&=-C\frac{3r(D-z)}{R_1^5}\end{aligned}\right\}\tag{8}$$

Substituting eqs. (8) into (7) and putting $R_1=a$, we obtain

$$\left.\begin{aligned}\sigma_{RR}&=\frac{2C}{a^3}\\ \sigma_{\theta\theta}&=-\frac{C}{a^3}\\ \sigma_{R\theta}&=0\end{aligned}\right\}\tag{9}$$

Now we assume that the normal stress at the spherical surface is balanced with the internal hydrostatic pressure $\Delta P$ (the compressive force is taken to be positive). With the aid of the first equation in (9) we obtain

$$C=\frac{a^3\Delta P}{2}\tag{10}$$

The deriving process of the factor $C$ shows that eq. (10) holds under the condition that $a\ll D$. The internal pressure has sometimes been discussed on the basis of eq. (10) by assuming some values of the radius $a$. $\Delta P$ and $a$ are essentially not independent in the Mogi model, so that the factor $C$ itself seems to have a more direct physical meaning. The quantity $C$ has a dimension of the moment of force, indicating the magnitude of the force source within a volcano.

Finally, the stress field components are given as follows by means of eqs. (4);

$$\left.\begin{aligned}\sigma_{rr}&=C\left\{\frac{2}{R_1^3}-\frac{3(z-D)^2}{R_1^5}+\frac{2(2\lambda+3\mu)}{\lambda+\mu}\frac{1}{R_2^3}-\frac{3(z+D)(11z+3D)}{R_2^5}+\frac{30z(z+D)^3}{R_2^7}\right\}\\ \sigma_{\varphi\varphi}&=C\left\{-\frac{1}{R_1^3}+\frac{\lambda-3\mu}{\lambda+\mu}\frac{1}{R_2^3}+\frac{1}{\lambda+\mu}\frac{6(z+D)(\mu z-\lambda D)}{R_2^5}\right\}\\ \sigma_{zz}&=C\left\{-\frac{1}{R_1^3}+\frac{3(z-D)^2}{R_1^5}+\frac{1}{R_2^3}+\frac{3(z+D)(5z-D)}{R_2^5}-\frac{30z(z+D)^3}{R_2^7}\right\}\\ \sigma_{zr}&=C3r\left\{\frac{z-D}{R_1^5}+\frac{3z+D}{R_2^5}-\frac{10z(z+D)^2}{R_2^7}\right\}\\ \sigma_{r\varphi}&=0\\ \sigma_{\varphi z}&=0\end{aligned}\right\}\tag{11}$$

## Stress-induced Magnetization

Magnetic properties of compressed rocks have been studied by many rock-magnetitians, and are summarized by NAGATA (1970) and STACEY and BANERJEE (1974). The induced magnetization due to the susceptibility and hard remanent magnetization such as TRM and CRM vary with the uniaxial compression ($\sigma>0$) in such a way as

$$\left.\begin{aligned} J^{//} &= \frac{J_0^{//}}{1+\beta\sigma} \cong J_0^{//}(1-\beta\sigma) \\ J^{\perp} &= \frac{J_0^{\perp}}{1-\frac{1}{2}\beta\sigma} \cong J_0^{\perp}\left(1+\frac{1}{2}\beta\sigma\right) \end{aligned}\right\} \tag{12}$$

where the signs // and $\perp$ indicate the component parallel and perpendicular to the applied stress respectively, while the subscript 0 denotes the value of unstressed state. $\beta$ is called the stress sensitivity having an order of $10^{-4}$ bar$^{-1}$. Empirical relations (12) are presumed to hold for the uniaxial tension ($\sigma<0$) by theoretical considerations.

Eqs. (12) were extended to the general three dimensional case by STACEY, BARR and ROBSON (1965). We may resolve the magnetization $J_0$ into orthogonal three components ($J_1$, $J_2$, $J_3$) in directions of principal stresses $\sigma_1$, $\sigma_2$, $\sigma_3$ and apply the relations (12) to each component. The stress-induced magnetization in each direction of the principal axis is then represented as

$$\left.\begin{aligned} &\Delta J_i \boldsymbol{e}_i = \beta J_i \left(\frac{\sigma_i+\sigma_k}{2}-\sigma_i\right)\boldsymbol{e}_i \\ &(i,\ j,\ k=1,\ 2,\ 3.\quad i\neq j\neq k) \end{aligned}\right\} \tag{13}$$

where $\{\boldsymbol{e}_1, \boldsymbol{e}_2, \boldsymbol{e}_3\}$ are the unit vectors in directions of principal stresses $\sigma_1$, $\sigma_2$, $\sigma_3$ at a point considered.

We are now to investigate principal stresses of the Mogi model's stress field. The stress components in eqs. (11) can be transformed into those in the Cartesian coordinates as follows,

$$\mathbf{T}=\begin{bmatrix} \sigma_{rr}\cos^2\varphi+\sigma_{\varphi\varphi}\sin^2\varphi\ , & (\sigma_{rr}-\sigma_{\varphi\varphi})\sin\varphi\cos\varphi, & \sigma_{zr}\cos\varphi \\ (\sigma_{rr}-\sigma_{\varphi\varphi})\sin\varphi\cos\varphi\ , & \sigma_{rr}\sin^2\varphi+\sigma_{\varphi\varphi}\cos^2\varphi\ , & \sigma_{zr}\sin\varphi \\ \sigma_{zr}\cos\varphi\ , & \sigma_{zr}\sin\varphi\ , & \sigma_{zz} \end{bmatrix} \tag{14}$$

Principal stresses are obtained by solving the eigen value equation of the matrix $\mathbf{T}$, namely

$$|\mathbf{T}-\sigma\mathbf{I}|=0 \tag{15}$$

where $\mathbf{I}$ is the unit matrix. The solutions are given in the following:

$$\left.\begin{aligned}\sigma_1&=\frac{\sigma_{rr}+\sigma_{zz}}{2}+\sqrt{\left(\frac{\sigma_{rr}-\sigma_{zz}}{2}\right)^2+\sigma_{zr}^2}\\ \sigma_2&=\sigma_{\varphi\varphi}\\ \sigma_3&=\frac{\sigma_{rr}+\sigma_{zz}}{2}-\sqrt{\left(\frac{\sigma_{rr}-\sigma_{zz}}{2}\right)^2+\sigma_{zr}^2}\end{aligned}\right\}\tag{16}$$

We may introduce an orthonormal matrix **P**, columns of which consist of eigen vectors of **T**. **P** satisfies the matrix equation:

$$\mathbf{P}^{-1}\mathbf{T}\mathbf{P}=\begin{bmatrix}\sigma_1 & 0 & 0\\ 0 & \sigma_2 & 0\\ 0 & 0 & \sigma_3\end{bmatrix}\tag{17}$$

,from which we obtain the following expression for **P**.

$$\left.\begin{aligned}\mathbf{P}&=\begin{bmatrix}\frac{\sigma_1-\sigma_{zz}}{\varDelta}\cos\varphi\,, & -\sin\varphi\,, & -\frac{\sigma_{zr}}{\varDelta}\cos\varphi\\ \frac{\sigma_1-\sigma_{zz}}{\varDelta}\sin\varphi\,, & \cos\varphi\,, & -\frac{\sigma_{zr}}{\varDelta}\sin\varphi\\ \frac{\sigma_{zr}}{\varDelta}\,, & 0\,, & \frac{\sigma_{rr}-\sigma_3}{\varDelta}\end{bmatrix}\\ &\text{where}\\ \varDelta&=\sqrt{(\sigma_1-\sigma_{zz})^2+\sigma_{zr}^2}=\sqrt{(\sigma_3-\sigma_{rr})^2+\sigma_{zr}^2}\end{aligned}\right\}\tag{18}$$

The matrix **P** defines the transformation of the original Cartesian coordinates $\{e_x, e_y, e_z\}$ into another set of Cartesian coordinates $\{e_1, e_2, e_3\}$, whose axes coincide with the principal axes of the stress tensor **T**. Direction cosines of $\sigma_1$, $\sigma_2$ and $\sigma_3$ axis are then given by components of the column vector of **P**. An arbitrary vector $J'=(J'_1, J'_2, J'_3)^t$ in the principal axes coordinates $\{e_1, e_2, e_3\}$ is related in a following way to the vector $J=(J_x, J_y, J_z)^t$, which is the same vector as $J'$ but is described in the original coordinate $\{e_x, e_y, e_z\}$,

$$J'=\mathbf{P}^{-1}J\tag{19}$$

For the convenience of following calculations, we may rewrite eq. (18) and put

$$\mathbf{P}^{-1}=\mathbf{P}^t=\begin{bmatrix}\lambda_1 & \mu_1 & \nu_1\\ \lambda_2 & \mu_2 & \nu_2\\ \lambda_3 & \mu_3 & \nu_3\end{bmatrix}$$

$$=\begin{bmatrix}\frac{b}{\sqrt{b^2+c^2}}\cos\varphi\,, & \frac{b}{\sqrt{b^2+c^2}}\sin\varphi\,, & \frac{c}{\sqrt{b^2+c^2}}\\ -\sin\varphi\,, & \cos\varphi\,, & 0\end{bmatrix}$$

$$\left[-\frac{c}{\sqrt{b^2+c^2}}\cos\varphi\,,\quad -\frac{c}{\sqrt{b^2+c^2}}\sin\varphi\,,\quad \frac{b}{\sqrt{b^2+c^2}}\right] \tag{20}$$

where

$$b=\frac{\sigma_{rr}-\sigma_{zz}}{2}+\sqrt{\left(\frac{\sigma_{rr}-\sigma_{zz}}{2}\right)^2+\sigma_{zr}^2}$$

$$c=\sigma_{zr}$$

We are in a position to obtain the stress-induced magnetization. Here the horizontal and the vertical magnetization cases will be dealt with separately.

(I) *In the case of Horizontal Magnetization in the x Direction*: we put $\boldsymbol{J}=J_H\boldsymbol{e}_x$ and substitute it into eq. (19);

$$\boldsymbol{J}'_H=\lambda_1 J_H\boldsymbol{e}_1+\lambda_2 J_H\boldsymbol{e}_2+\lambda_3 J_H\boldsymbol{e}_3 \tag{21}$$

Applying the empirical formulae of piezomagnetism (13) to the elementary volume $dV=dxdydz$ at a point $(x, y, z)$, we obtain the increments of magnetization in the principal axis directions as follows,

$$\left.\begin{aligned} d\boldsymbol{M}_1&=\beta T_1\lambda_1 J_H dV\boldsymbol{e}_1\\ d\boldsymbol{M}_2&=\beta T_2\lambda_2 J_H dV\boldsymbol{e}_2\\ d\boldsymbol{M}_3&=\beta T_3\lambda_3 J_H dV\boldsymbol{e}_3 \end{aligned}\right\} \tag{22}$$

where

$$\left.\begin{aligned} T_1&=\frac{\sigma_2+\sigma_3}{2}-\sigma_1\\ T_2&=\frac{\sigma_1+\sigma_3}{2}-\sigma_2\\ T_3&=\frac{\sigma_1+\sigma_2}{2}-\sigma_3 \end{aligned}\right\} \tag{23}$$

With the aid of the following relations derived from eq. (19),

$$\left.\begin{aligned} \boldsymbol{e}_1&=\lambda_1\boldsymbol{e}_x+\mu_1\boldsymbol{e}_y+\nu_1\boldsymbol{e}_z\\ \boldsymbol{e}_2&=\lambda_2\boldsymbol{e}_x+\mu_2\boldsymbol{e}_y+\nu_2\boldsymbol{e}_z\\ \boldsymbol{e}_3&=\lambda_3\boldsymbol{e}_x+\mu_3\boldsymbol{e}_y+\nu_3\boldsymbol{e}_z \end{aligned}\right\} \tag{24}$$

we obtain the total increment of magnetization $d\boldsymbol{M}_H$ at a point as;

$$d\boldsymbol{M}_H=d\boldsymbol{M}_1+d\boldsymbol{M}_2+d\boldsymbol{M}_3=\beta J_H(S_{xx}\boldsymbol{e}_x+S_{xy}\boldsymbol{e}_y+S_{xz}\boldsymbol{e}_z)dxdydz \tag{25}$$

where

$$\left.\begin{aligned} S_{xx} &= \lambda_1^2 T_1 + \lambda_2^2 T_2 + \lambda_3^2 T_3 \\ S_{xy} &= \lambda_1 \mu_1 T_1 + \lambda_2 \mu_2 T_2 + \lambda_3 \mu_3 T_3 \\ S_{xz} &= \lambda_1 \nu_1 T_1 + \lambda_2 \nu_2 T_2 + \lambda_3 \nu_3 T_3 \end{aligned}\right\} \tag{26}$$

Eq. (25) shows that $\beta J_H S_{xx}$, *etc.* are the stress-induced magnetization in the $x$, $y$ and $z$ direction respectively for a given horizontal magnetization.

(II) *In the case of Vertical Magnetization*:
putting $\boldsymbol{J} = J_V \boldsymbol{e}_z$ in eq. (19), we obtain

$$\boldsymbol{J}_V' = \nu_1 J_V \boldsymbol{e}_1 + \nu_2 J_V \boldsymbol{e}_2 + \nu_3 J_V \boldsymbol{e}_3 \tag{27}$$

The incremental magnetizations in the principal axis direction are in this case as follows,

$$\left.\begin{aligned} d\boldsymbol{M}_1 &= \beta T_1 \nu_1 J_V d\,V \boldsymbol{e}_1 \\ d\boldsymbol{M}_2 &= \beta T_2 \nu_2 J_V d\,V \boldsymbol{e}_2 \\ d\boldsymbol{M}_3 &= \beta T_3 \nu_3 J_V d\,V \boldsymbol{e}_3 \end{aligned}\right\} \tag{28}$$

The total stress-induced magnetization $d\boldsymbol{M}_V$ in the vertical magnetization case is given by

$$d\boldsymbol{M}_V = \beta J_V (S_{zx}\boldsymbol{e}_x + S_{zy}\boldsymbol{e}_y + S_{zz}\boldsymbol{e}_z) dxdydz \tag{29}$$

where

$$\left.\begin{aligned} S_{zx} &= \lambda_1 \nu_1 T_1 + \lambda_2 \nu_2 T_2 + \lambda_3 \nu_3 T_3 \\ S_{zy} &= \mu_1 \nu_1 T_1 + \mu_2 \nu_2 T_2 + \mu_3 \nu_3 T_3 \\ S_{zz} &= \nu_1^2 T_1 + \nu_2^2 T_2 + \nu_3^2 T_3 \end{aligned}\right\} \tag{30}$$

$\beta J_V S_{zx}$, *etc.* are the stress-induced magnetization in the $x$, $y$ and $z$ direction for a given vertical magnetization.

Substituting eqs. (16), (20) and (23) into (26) and (30), we find each component of the stress-induced magnetization in the form of linear combinations of stress components:

$$\left.\begin{aligned} S_{xx} &= \frac{1}{2}(\sigma_{rr} + \sigma_{zz} - 2\sigma_{\varphi\varphi}) - \frac{3}{2}(\sigma_{rr} - \sigma_{\varphi\varphi})\cos^2\varphi \\ S_{xy} &= -\frac{3}{2}(\sigma_{rr} - \sigma_{\varphi\varphi})\sin\varphi\cos\varphi \\ S_{xz} &= -\frac{3}{2}\sigma_{zr}\cos\varphi \\ S_{zx} &= S_{xz} \\ S_{zy} &= -\frac{3}{2}\sigma_{zr}\sin\varphi \end{aligned}\right\} \tag{31}$$

$$S_{zz}=\frac{1}{2}(\sigma_{rr}+\sigma_{\varphi\varphi}-2\sigma_{zz})$$

It should be emphasized that eqs. (31) hold for any axi-symmetric problems with respect to the $z$ axis, because these formulae are deduced solely on the basis of general symmetric properties of the stress tensor and $\sigma_{z\varphi}=\sigma_{r\varphi}=0$.

Finally, the stress-induced magnetization for the Mogi model is given in a concrete form as:

$$\begin{aligned}
S_{xx}=&\frac{3}{2}\frac{1}{R_1^3}+\frac{3\lambda+13\mu}{2(\lambda+\mu)}\frac{1}{R_2^3}-3\left(\frac{3\lambda+5\mu}{\lambda+\mu}z+\frac{2\mu}{\lambda+\mu}D\right)\frac{z+D}{R_2^5}\\
&-\frac{9}{2}\frac{x^2}{r^2}\left\{\frac{1}{R_1^3}-\frac{(z-D)^2}{R_1^5}+\frac{\lambda+3\mu}{\lambda+\mu}\frac{1}{R_2^3}\right.\\
&\left.-\left(\frac{11\lambda+13\mu}{\lambda+\mu}z+\frac{\lambda+3\mu}{\lambda+\mu}D\right)\frac{z+D}{R_2^5}+\frac{10z(z+D)^3}{R_2^7}\right\}\\
S_{xy}=&-\frac{9}{2}\frac{xy}{r^2}\left\{\frac{1}{R_1^3}-\frac{(z-D)^2}{R_1^5}+\frac{\lambda+3\mu}{\lambda+\mu}\frac{1}{R_2^3}\right.\\
&\left.-\left(\frac{11\lambda+13\mu}{\lambda+\mu}z+\frac{\lambda+3\mu}{\lambda+\mu}D\right)\frac{z+D}{R_2^5}+\frac{10z(z+D)^3}{R_2^7}\right\}
\end{aligned}$$

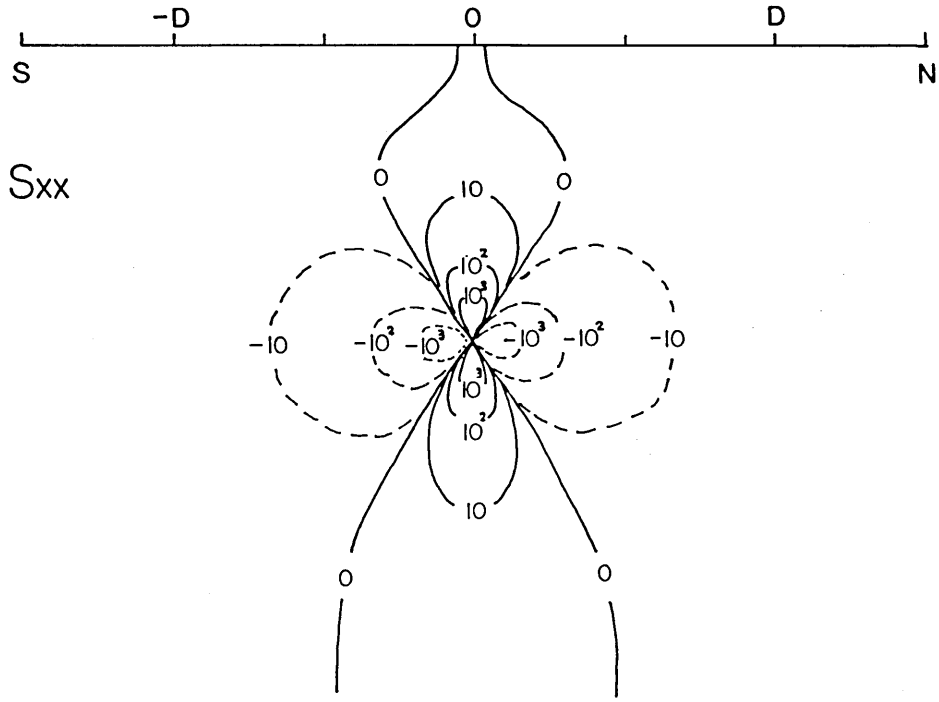


(a)

Fig. 2(a). Stress-induced magnetization $S_{xx}$ within the $N$-$S$ meridian plane in unit of $kJ_0C/D^3$. $\lambda=\mu$ is assumed.

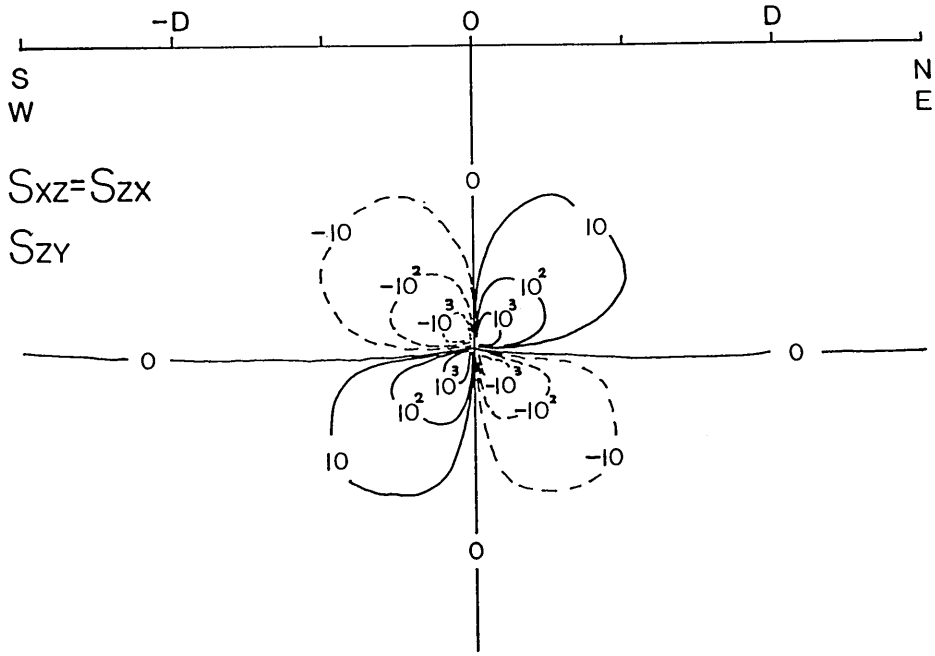


(b)

Fig. 2(b). Stress-induced magnetization $S_{xz}=S_{zx}$ within the *N-S* meridian plane. This figure also represents the $S_{zy}$ component within the *E-W* meridian plane.

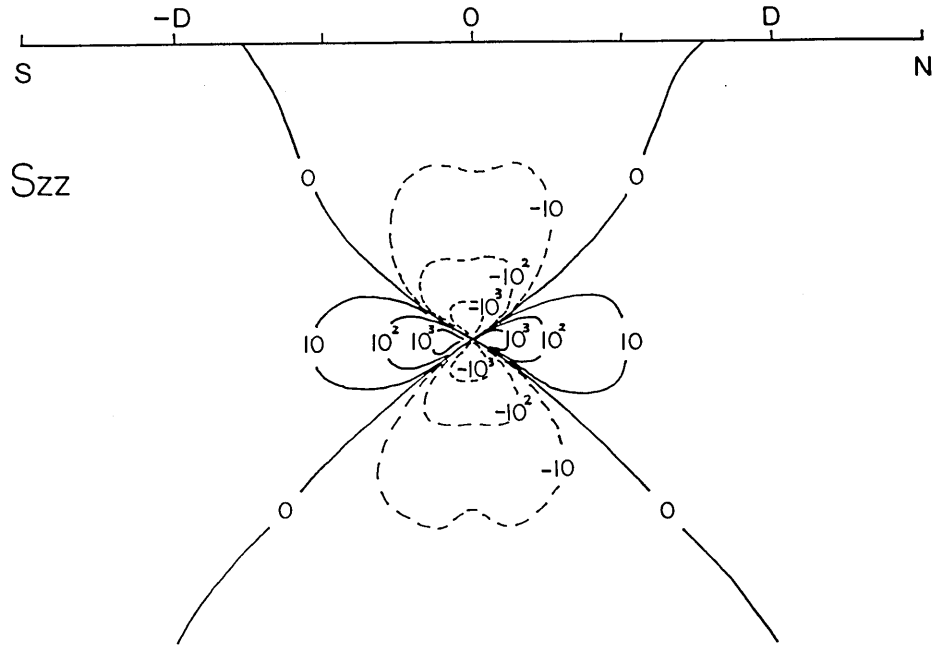


(c)

Fig. 2(c). Stress-induced magnetization $S_{zz}$ within the *N-S* meridian plane.

$$\left.\begin{aligned}
S_{xz}&=S_{zx}\\
&=-\frac{9}{2}x\left\{\frac{z-D}{R_1^5}+\frac{3z+D}{R_2^5}-\frac{10z(z+D)^2}{R_2^7}\right\}\\
S_{yz}&=-\frac{9}{2}y\left\{\frac{z-D}{R_1^5}+\frac{3z+D}{R_2^5}-\frac{10z(z+D)^2}{R_2^7}\right\}\\
S_{zz}&=\frac{3}{2}\frac{1}{R_1^3}-\frac{9}{2}\frac{(z-D)^2}{R_1^5}+\frac{1}{2}\frac{3\lambda+\mu}{\lambda+\mu}\frac{1}{R_2^3}\\
&\quad-\frac{3}{2}\left(\frac{21\lambda+19\mu}{\lambda+\mu}z+\frac{3\lambda+\mu}{\lambda+\mu}D\right)\frac{z+D}{R_2^5}+\frac{45z(z+D)^3}{R_2^7}
\end{aligned}\right\}\tag{32}$$

In Figs. 2(a), 2(b) and 2(c) are illustrated $S_{xx}$, $S_{xz}=S_{zx}$ and $S_{zz}$ in the $N-S$ meridian plane including the $z$ axis. We may regard Fig. 2(b) as the distribution of $S_{zy}$ in the $E-W$ meridian plane. Although the symmetric distribution around the dilation center is the most dominant, we can clearly observe that the symmetry with respect to the plane $z=D$ breaks especially near the free surface $z=0$.

## Piezomagnetic Field

The potential of the magnetic field at $(x, y, z)$ produced by a magnetic dipole moment $dM$ at $(x', y', z')$ is given by the dipole law of force as;

$$\left.\begin{aligned}
dW&=\left(\frac{x-x'}{r'^3}e_x+\frac{y-y'}{r'^3}e_y+\frac{z-z'}{r'^3}e_z\right)\cdot dM\\
&\text{where}\\
r'&=\sqrt{(x-x')^2+(y-y')^2+(z-z')^2}
\end{aligned}\right\}\tag{33}$$

Substituting eq. (25) and (29) into (33), we obtain

$$\left.\begin{aligned}
dW_H&=C\beta J_H(S_{xx}\cdot U'_x+S_{xy}\cdot U'_y+S_{xz}\cdot U'_z)dxdydz\\
dW_V&=C\beta J_V(S_{zx}\cdot U'_x+S_{zy}\cdot U'_y+S_{zz}\cdot U'_z)dxdydz
\end{aligned}\right\}\tag{34}$$

where

$$\left.\begin{aligned}
U'_x&=\frac{x-x'}{r'^3}\\
U'_y&=\frac{y-y'}{r'^3}\\
U'_z&=\frac{z-z'}{r'^3}
\end{aligned}\right\}\tag{35}$$

By integrating eqs. (34) over the whole magnetized area, the piezomagnetic field potential of the Mogi model should be obtained even

when $\beta$, $J_H$ and $J_V$ are functions of position. We consider here a very limited case that the upper part of the earth's crust is uniformly magnetized from surface $z'=0$ to a depth $z'=H$, the $x$ axis being taken in the magnetic north direction. The magnetic potential can be given as follows;

$$\left.\begin{aligned} W_H &= C\beta J_H \int_0^H dz' \iint_{-\infty}^{\infty} (S_{xx}\cdot U'_x + S_{xy}\cdot U'_y + S_{xz}\cdot U'_z)dx'dy' \\ W_V &= C\beta J_V \int_0^H dz' \iint_{-\infty}^{\infty} (S_{zx}\cdot U'_x + S_{zy}\cdot U'_y + S_{zz}\cdot U'_z)dx'dy' \end{aligned}\right\} \tag{36}$$

The integrals with respect to $x'$ and $y'$ in eqs. (36) have a form of the convolution integral. A useful theorem could be employed here, with regard to the Fourier transforms of the convolution integral. Let $f^*(\xi, \eta)$ and $g^*(\xi, \eta)$ denote Fourier transforms of functions $f(x, y)$ and $g(x, y)$ respectively. The convolution of the present two functions is defined as

$$\left.\begin{aligned} h(x, y) &= \iint_{-\infty}^{\infty} f(x, y)g(x-x', y-y')dx'dy' \\ &= \iint_{-\infty}^{\infty} g(x, y)f(x-x', y-y')dx'dy' \end{aligned}\right\} \tag{37}$$

The Fourier transform of the convolution $h(x, y)$ is given by

$$h^*(\xi, \eta) = 2\pi f^*(\xi, \eta)g^*(\xi, \eta) \tag{38}$$

The double Fourier integral transform and its inverse are defined in this paper in a form;

$$\left.\begin{aligned} f^*(\xi, \eta) &= \frac{1}{2\pi}\iint_{-\infty}^{\infty} f(x, y)e^{-i(\xi x+\eta y)}dxdy \\ f(x, y) &= \frac{1}{2\pi}\iint_{-\infty}^{\infty} f^*(\xi, \eta)e^{i(\xi x+\eta y)}d\xi d\eta \end{aligned}\right\} \tag{39}$$

With the aid of this theorem, the following integrals can be evaluated;

$$\left.\begin{aligned} w_H &= \iint_{-\infty}^{\infty} (S_{xx}\cdot U'_x + S_{xy}\cdot U'_y + S_{xz}\cdot U'_z)dx'dy' \\ w_V &= \iint_{-\infty}^{\infty} (S_{zx}\cdot U'_x + S_{zy}\cdot U'_y + S_{zz}\cdot U'_z)dx'dy' \end{aligned}\right\} \tag{40}$$

We must first obtain the Fourier transforms of $S_{xx}$, $S_{xy}$, etc. and $U_x$, $U_y$ and $U_z$ with respect to $x$ and $y$. All the fundamental formulae of the Fourier transforms necessary for the present purpose are listed in Table 1. These are derived briefly in the Appendix, although some

Table 1. Fourier transforms.

| | $f(x,\ y)$ | $f^*(\xi,\ \eta)=\frac{1}{2\pi}\iint_{-\infty}^{\infty} f(x,\ y)e^{-i(\xi x+\eta y)}dxdy$ |
|---|---|---|
| $F-1$ | $\frac{1}{\rho^3}$ | $\frac{1}{\zeta}e^{-\alpha\zeta}$ |
| $F-2$ | $\frac{x}{\rho^3}$ | $-i\frac{\xi}{\alpha}e^{-\alpha\zeta}$ |
| $F-3$ | $\frac{y}{\rho^3}$ | $-i\frac{\eta}{\alpha}e^{-\alpha\zeta}$ |
| $F-4$ | $\frac{1}{\rho^5}$ | $\frac{1}{3\zeta^2}\left(\alpha+\frac{1}{\zeta}\right)e^{-\alpha\zeta}$ |
| $F-5$ | $\frac{x}{\rho^5}$ | $-\frac{1}{3}\frac{i\xi}{\zeta}e^{-\alpha\zeta}$ |
| $F-6$ | $\frac{y}{\rho^5}$ | $-\frac{1}{3}\frac{i\eta}{\zeta}e^{-\alpha\zeta}$ |
| $F-7$ | $\frac{1}{\rho^7}$ | $\frac{1}{15\zeta^3}\left(\alpha^2+\frac{3\alpha}{\zeta}+\frac{3}{\zeta^2}\right)e^{-\alpha\zeta}$ |
| $F-8$ | $\frac{x}{\rho^7}$ | $-\frac{1}{15\zeta^2}\left(i\xi\alpha+i\xi\frac{1}{\zeta}\right)e^{-\alpha\zeta}$ |
| $F-9$ | $\frac{y}{\rho^7}$ | $-\frac{1}{15\zeta^2}\left(i\eta\alpha+i\eta\frac{1}{\zeta}\right)e^{-\alpha\zeta}$ |
| $F-10$ | $\frac{x^2}{r^2}\frac{1}{\rho^3}$ | $\frac{1}{\zeta^3}\cdot\frac{\eta^2-\xi^2}{\alpha^4}+\frac{1}{\zeta}\left(\frac{\xi^2-\eta^2}{\alpha^4}\cdot\frac{1}{\zeta^2}+\frac{\xi^2-\eta^2}{\alpha^3}\cdot\frac{1}{\zeta}+\frac{\xi^2}{\alpha^2}\right)e^{-\alpha\zeta}$ |
| $F-11$ | $\frac{x^2}{r^2}\frac{1}{\rho^5}$ | $\frac{1}{\zeta^5}\cdot\frac{\eta^2-\xi^2}{\alpha^4}+\frac{1}{\zeta^2}\left(\frac{\xi^2-\eta^2}{\alpha^4}\cdot\frac{1}{\zeta^3}+\frac{\xi^2-\eta^2}{\alpha^3}\cdot\frac{1}{\zeta^2}+\frac{2\xi^2-\eta^2}{3\alpha^2}\cdot\frac{1}{\zeta}+\frac{\xi^2}{3\alpha}\right)e^{-\alpha\zeta}$ |
| $F-12$ | $\frac{x^2}{r^2}\frac{1}{\rho^7}$ | $\frac{1}{\zeta^7}\cdot\frac{\eta^2-\xi^2}{\alpha^4}+\frac{1}{\zeta^3}\left(\frac{\xi^2-\eta^2}{\alpha^4}\cdot\frac{1}{\zeta^4}+\frac{\xi^2-\eta^2}{\alpha^3}\cdot\frac{1}{\zeta^3}+\frac{3\xi^2-2\eta^2}{5\alpha^2}\cdot\frac{1}{\zeta^2}+\frac{4\xi^2-\eta^2}{15\alpha}\cdot\frac{1}{\zeta}+\frac{\xi^2}{15}\right)e^{-\alpha\zeta}$ |
| $F-13$ | $\frac{xy}{r^2}\frac{1}{\rho^3}$ | $-\frac{1}{\zeta^3}\frac{2\xi\eta}{\alpha^4}+\frac{1}{\zeta}\left(\frac{2\xi\eta}{\alpha^4}\cdot\frac{1}{\zeta^2}+\frac{2\xi\eta}{\alpha^3}\cdot\frac{1}{\zeta}+\frac{\xi\eta}{\alpha^2}\right)e^{-\alpha\zeta}$ |
| $F-14$ | $\frac{xy}{r^2}\frac{1}{\rho^5}$ | $-\frac{1}{\zeta^5}\frac{2\xi\eta}{\alpha^4}+\frac{1}{\zeta^2}\left(\frac{2\xi\eta}{\alpha^4}\cdot\frac{1}{\zeta^3}+\frac{2\xi\eta}{\alpha^3}\cdot\frac{1}{\zeta^2}+\frac{\xi\eta}{\alpha^2}\cdot\frac{1}{\zeta}+\frac{1}{3}\cdot\frac{\xi\eta}{\alpha}\right)e^{-\alpha\zeta}$ |
| $F-15$ | $\frac{xy}{r^2}\frac{1}{\rho^7}$ | $-\frac{1}{\zeta^7}\frac{2\xi\eta}{\alpha^4}+\frac{1}{\zeta^3}\left(\frac{2\xi\eta}{\alpha^4}\cdot\frac{1}{\zeta^4}+\frac{2\xi\eta}{\alpha^3}\cdot\frac{1}{\zeta^3}+\frac{\xi\eta}{\alpha^2}\cdot\frac{1}{\zeta^2}+\frac{\xi\eta}{3\alpha}\cdot\frac{1}{\zeta}+\frac{\xi\eta}{15}\right)e^{-\alpha\zeta}$ |

$$\rho=\sqrt{x^2+y^2+\zeta^2}\quad(\zeta>0)\ ,\quad \alpha=\sqrt{\xi^2+\eta^2}$$

of them are easily found in the texbook (e.g. WATSON 1922).

The Fourier transforms of $S_{xx}$ and so on are obtained as follows;

$$\left.\begin{aligned}
S^*_{xx}&=\frac{3}{2}\frac{\xi^2}{\alpha}e^{-\alpha\zeta_1}+\left(-\frac{2\mu}{\lambda+\mu}\alpha+\frac{3}{2}\frac{\lambda+3\mu}{\lambda+\mu}\frac{\xi^2}{\alpha}-3\xi^2z'\right)e^{-\alpha\zeta_2}\\
S^*_{xy}&=\frac{3}{2}\frac{\xi\eta}{\alpha}e^{-\alpha\zeta_1}+\left(\frac{3}{2}\frac{\lambda+3\mu}{\lambda+\mu}\frac{\xi\eta}{\alpha}-3\xi\eta z'\right)e^{-\alpha\zeta_2}\\
S^*_{xz}&=\mp\frac{3}{2}i\xi e^{-\alpha\zeta_1}+\frac{3}{2}i\xi(1-2\alpha z')e^{-\alpha\zeta_2}\quad(z'\lesseqgtr D)\\
S^*_{zx}&=S^*_{xz}\\
S^*_{zy}&=\mp\frac{3}{2}i\eta e^{-\alpha\zeta_1}+\frac{3}{2}i\eta(1-2\alpha z')e^{-\alpha\zeta_2}\quad(z'\lesseqgtr D)
\end{aligned}\right\}\tag{41}$$

$$S_{zz}^{*}=-\frac{3}{2}\alpha e^{-\alpha\zeta_1}+\left(3\alpha^2 z'-\frac{3\lambda+\mu}{2(\lambda+\mu)}\alpha\right)e^{-\alpha\zeta_2}$$

where

$$\left.\begin{aligned}\zeta_1&=|z'-D|\\ \zeta_2&=z'+D\end{aligned}\right\} \tag{42}$$

while Fourier transforms of $U_x$, $U_y$ and $U_z$ are given as

$$\left.\begin{aligned}U_x^{*}&=-\frac{i\xi}{\alpha}e^{-\alpha\zeta}\\ U_y^{*}&=-\frac{i\eta}{\alpha}e^{-\alpha\zeta}\\ U_z^{*}&=-e^{-\alpha\zeta}\end{aligned}\right\} \tag{43}$$

where

$$\zeta=z'-z \tag{44}$$

Combining (41) and (43) through the basic relation (38), we obtain Fourier transforms of $w_H$ and $w_V$;

$$\left.\begin{aligned}\frac{w_H^{*}}{2\pi}&=S_{xx}^{*}\cdot U_x^{*}+S_{xy}^{*}\cdot U_y^{*}+S_{xz}^{*}\cdot U_z^{*}\\ &=\left(-\frac{3\lambda+4\mu}{\lambda+\mu}i\xi+6i\xi\alpha z'\right)e^{-\alpha(2z'+D-z)}\\ &\quad+\begin{cases}0 & (0<z'<D)\\ -3i\xi e^{-\alpha(2z'-D-z)} & (D<z')\end{cases}\\ \frac{w_V^{*}}{2\pi}&=S_{zx}^{*}\cdot U_x^{*}+S_{zy}^{*}\cdot U_y^{*}+S_{zz}^{*}\cdot U_z^{*}\\ &=\left(\frac{3\lambda+2\mu}{\lambda+\mu}\alpha-6\alpha^2 z'\right)e^{-\alpha(2z'+D-z)}\\ &\quad+\begin{cases}0 & (0<z'<D)\\ 3\alpha e^{-\alpha(2z'-D-z)} & (D<z')\end{cases}\end{aligned}\right\} \tag{45}$$

Performing the inverse transformation, we can find $w_H$ and $w_V$ as functions of $z'$. Inverse Fourier transforms of some fundamental functions are listed in Table 2. These may be easily derived from the formula (A7) in the Appendix by differentiation with respect to $\zeta$ and $x$. $w_H$ and $w_V$ are given as follows;

$$\left.\begin{aligned}\frac{w_H}{2\pi}&=\frac{3\lambda+4\mu}{\lambda+\mu}\frac{3xz_2}{\rho_2^5}+18xz'\left(\frac{1}{\rho_2^5}-\frac{5z_2^2}{\rho_2^5}\right)\\ &=\begin{cases}0 & (0<z'<D)\\ \dfrac{9xz_1}{\rho_1^5} & (D<z')\end{cases}\end{aligned}\right|$$

$$\left.\begin{aligned}\frac{w_V}{2\pi}=&\frac{3\lambda+2\mu}{\lambda+\mu}\left(-\frac{1}{\rho_2^3}+\frac{3z_2^2}{\rho_2^5}\right)-6z'\left(-\frac{9z_2}{\rho_2^5}+\frac{15z_2^3}{\rho_2^7}\right)\\&+\begin{cases}0 & (0<z'<D)\\ -\dfrac{3}{\rho_1^3}+\dfrac{9z_1^2}{\rho_1^5} & (D<z')\end{cases}\\ \text{where}\quad & z_1=2z'-D-z\\ & z_2=2z'+D-z\\ & \rho_1=\sqrt{x^2+y^2+z_1^2}\\ & \rho_2=\sqrt{x^2+y^2+z_2^2}\end{aligned}\right\}\tag{46}$$

Table 2. Inverse Fourier transforms.

| | $f^*(\xi,\ \eta)$ | $f(x,\ y)=\frac{1}{2\pi}\iint_{-\infty}^{\infty} f^*(\xi,\ \eta)e^{i(\xi x+\eta y)}d\xi d\eta$ |
|---|---|---|
| $F-16$ | $\frac{i\xi}{\alpha}e^{-\alpha\zeta}$ | $-\frac{x}{\rho^3}$ |
| $F-17$ | $i\xi e^{-\alpha\zeta}$ | $-\frac{3x\zeta}{\rho^5}$ |
| $F-18$ | $i\xi\alpha e^{-\alpha\zeta}$ | $\frac{3x}{\rho^5}-\frac{15x\zeta^2}{\rho^7}$ |
| $F-19$ | $e^{-\alpha\zeta}$ | $\frac{\zeta}{\rho^3}$ |
| $F-20$ | $\alpha e^{-\alpha\zeta}$ | $-\frac{1}{\rho^3}+\frac{3\zeta^2}{\rho^5}$ |
| $F-21$ | $\alpha^2 e^{-\alpha\zeta}$ | $-\frac{9\zeta}{\rho^5}+\frac{15\zeta^3}{\rho^7}$ |

$\rho=\sqrt{x^2+y^2+\zeta^2}\quad(\zeta>0),\quad \alpha=\sqrt{\xi^2+\eta^2}$

There appears an interesting feature in eq. (46). The last term of either $w_H$ or $w_V$ represents the major contribution from magnetization changes produced by the center of dilatation itself, while the first and second terms imply an additional one caused by the existence of the surface boundary. Major magnetization changes induced in a horizontal plane within the region $0<z'<D$ completely cancel each other's magnetic field as a whole; they produce no magnetic field in the free space. On the contrary, the lower region ($z'>D$) contributes to the magnetic field in free space considerably. The difference comes from the antisymmetric shear stress distribution of the major component with respect to a plane $z'=D$, namely the term $(z-D)/R_1^5$ in eqs. (11).

The magnetic potential might be found by integrating $w_H$ and $w_V$ with respect to $z'$;

$$\left.\begin{aligned} W_H &= 2\pi C\int \beta J_H w_H dz' \\ W_V &= 2\pi C\int \beta J_V w_V dz' \end{aligned}\right\} \tag{47}$$

It should be noticed that eqs. (47) hold even for a layered earth in which $\beta$, $J_H$ and $J_V$ are arbitrary functions of depth only.

We are concerned here with the most simple case of uniform stress sensitivity and magnetization. Since integrals involved in (47) are rather complicated, we will make a slightly different approach to the total magnetic potential. $w_H^*$ and $w_V^*$ are integrated first with respect to $z'$ from 0 to a depth $H$, which results in

$$\left.\begin{aligned} \frac{W_H^*}{C_H} &= -\frac{\mu}{2(\lambda+\mu)}\frac{i\xi}{\alpha}(e^{-\alpha D_1}-e^{-\alpha D_3})-3Hi\xi e^{-\alpha D_3} \\ &+\begin{cases} 0 & (D\geqq H) \\ -\dfrac{3}{2}\dfrac{i\xi}{\alpha}(e^{-\alpha D_1}-e^{-\alpha D_2}) & (H>D) \end{cases} \\ \frac{W_V^*}{C_V} &= -\frac{\mu}{2(\lambda+\mu)}(e^{-\alpha D_1}-e^{-\alpha D_3})+3H\alpha e^{-\alpha D_3} \\ &+\begin{cases} 0 & (D\geqq H) \\ \dfrac{3}{2}(e^{-\alpha D_1}-e^{-\alpha D_2}) & (H>D) \end{cases} \end{aligned}\right\} \tag{48}$$

where

$$D_1=D-z,\quad D_2=2H-D-z,\quad D_3=2H+D-z \tag{49}$$

and

$$C_H=2\pi\beta J_H C,\quad C_V=2\pi\beta J_V C \tag{50}$$

The inverse Fourier transform of $W_H^*$ and $W_V^*$ will be obtained again by making use of formulae in Table 2;

$$\left.\begin{aligned} \frac{W_H}{C_H} &= \frac{\mu}{2(\lambda+\mu)}\frac{x}{\rho_1^3}-\frac{\mu}{2(\lambda+\mu)}\frac{x}{\rho_3^3}+\frac{9HxD_3}{\rho_3^5} \\ &+\begin{cases} 0 & (D>H) \\ \dfrac{3}{2}\left(\dfrac{x}{\rho_1^3}-\dfrac{x}{\rho_2^3}\right) & (H\geqq D) \end{cases} \\ \frac{W_V}{C_V} &= -\frac{\mu}{2(\lambda+\mu)}\frac{D_1}{\rho_1^3}+\frac{\mu}{2(\lambda+\mu)}\frac{D_3}{\rho_3^3}+3H\left(-\frac{1}{\rho_3^3}+\frac{3D_3^2}{\rho_3^5}\right) \end{aligned}\right\} \tag{51}$$

$$+\begin{cases} 0 & (D>H) \\ \dfrac{3}{2}\left(\dfrac{D_1}{\rho_1^3}-\dfrac{D_2}{\rho_2^3}\right) & (H\geqq D) \end{cases}$$

where

$$\left.\begin{aligned} \rho_1&=\sqrt{x^2+y^2+D_1^2} \\ \rho_2&=\sqrt{x^2+y^2+D_2^2} \\ \rho_3&=\sqrt{x^2+y^2+D_3^2} \end{aligned}\right\} \tag{52}$$

The piezomagnetic field due to the Mogi model proves to be of a very simple form. It consists of magnetic fields produced by dipoles centered at $(0, 0, D)$, $(0, 0, 2H-D)$ and $(0, 0, 2H+D)$ and a quadrupole at $(0, 0, 2H+D)$. An extreme case that $H$ approaches to infinity reduces to

$$\left.\begin{aligned} \frac{W_H}{C_H}&=\frac{3\lambda+4\mu}{2(\lambda+\mu)}\frac{x}{\rho_1^3} \\ \frac{W_V}{C_V}&=-\frac{3\lambda+2\mu}{2(\lambda+\mu)}\frac{z-D}{\rho_1^3} \end{aligned}\right\} \tag{53}$$

These are a northward horizontal dipole along the $x$ axis and an upward dipole along the $z$ axis both placed at the dilation center.

The magnetic field in the free space will be given by means of a well-known formula $\boldsymbol{H}=-grad\ W$. Writing the $x$-, $y$- and $z$-component due to the horizontal and vertical uniform magnetization $(X_H, Y_H, Z_H)$ and $(X_V, Y_V, Z_V)$ respectively, we arrive at the final expressions for the piezomagnetic field accompanying the Mogi model;

$$\frac{X_H}{C_H}=-\frac{\mu}{2(\lambda+\mu)}\left(\frac{1}{\rho_1^3}-\frac{3x^2}{\rho_1^5}\right)+\frac{\mu}{2(\lambda+\mu)}\left(\frac{1}{\rho_3^3}-\frac{3x^2}{\rho_3^5}\right)-9HD_3\left(\frac{1}{\rho_3^5}-\frac{5x^2}{\rho_3^7}\right)$$

$$+\begin{cases} 0 & (D\geqq H) \\ -\dfrac{3}{2}\left(\dfrac{1}{\rho_1^3}-\dfrac{3x^2}{\rho_1^5}\right)+\dfrac{3}{2}\left(\dfrac{1}{\rho_2^3}-\dfrac{3x^2}{\rho_2^5}\right) & (H>D) \end{cases}$$

$$\frac{Y_H}{C_H}=\frac{3\mu}{2(\lambda+\mu)}\frac{xy}{\rho_1^5}-\frac{3\mu}{2(\lambda+\mu)}\frac{xy}{\rho_3^5}+45HD_3\frac{xy}{\rho_3^7}$$

$$+\begin{cases} 0 & (D\geqq H) \\ \dfrac{9}{2}\dfrac{xy}{\rho_1^5}-\dfrac{9}{2}\dfrac{xy}{\rho_2^5} & (H>D) \end{cases}$$

$$\frac{Z_H}{C_H}=-\frac{3\mu}{2(\lambda+\mu)}\frac{xD_1}{\rho_1^5}+\frac{3\mu}{2(\lambda+\mu)}\frac{xD_3}{\rho_3^5}+9HD_3x\left(\frac{1}{\rho_3^5}-\frac{5D_3^2}{\rho_3^7}\right)$$

$$
\left.
\begin{aligned}
&+\begin{cases} 0 & (D \geqq H) \\ -\dfrac{9}{2}\dfrac{xD_1}{\rho_1^5}+\dfrac{9}{2}\dfrac{xD_3}{\rho_2^5} & (H>D) \end{cases} \\
\frac{X_V}{C_V}&=-\frac{3\mu}{2(\lambda+\mu)}\frac{xD_1}{\rho_1^5}+\frac{3\mu}{2(\lambda+\mu)}\frac{xD_3}{\rho_3^5}-9HD_3x\left(\frac{1}{\rho_3^5}-\frac{5D_3^2}{\rho_3^7}\right) \\
&+\begin{cases} 0 & (D \geqq H) \\ \dfrac{9}{2}\dfrac{xD_1}{\rho_1^5}-\dfrac{9}{2}\dfrac{xD_2}{\rho_2^5} & (H>D) \end{cases} \\
\frac{Y_V}{C_V}&=-\frac{3\mu}{2(\lambda+\mu)}\frac{yD_1}{\rho_1^5}+\frac{3\mu}{2(\lambda+\mu)}\frac{yD_3}{\rho_3^5}-9HD_3y\left(\frac{1}{\rho_3^5}-\frac{5D_3^2}{\rho_3^7}\right) \\
&+\begin{cases} 0 & (D \geqq H) \\ \dfrac{9}{2}\dfrac{yD_1}{\rho_1^5}-\dfrac{9}{2}\dfrac{yD_2}{\rho_2^5} & (H>D) \end{cases} \\
\frac{Z_V}{C_V}&=-\frac{\mu}{2(\lambda+\mu)}\left(\frac{1}{\rho_1^3}-\frac{3D_1^2}{\rho_1^5}\right)+\frac{\mu}{2(\lambda+\mu)}\left(\frac{1}{\rho_3^3}-\frac{3D_3^2}{\rho_3^5}\right)+9HD_3\left(\frac{3}{\rho_3^5}-\frac{5D_3^2}{\rho_3^7}\right) \\
&+\begin{cases} 0 & (D \geqq H) \\ \dfrac{3}{2}\left(\dfrac{1}{\rho_1^3}-\dfrac{3D_1^2}{\rho_1^5}\right)-\dfrac{3}{2}\left(\dfrac{1}{\rho_2^3}-\dfrac{3D_2^2}{\rho_2^5}\right) & (H>D) \end{cases}
\end{aligned}
\right\} \tag{54}
$$

When the depth of Currie point isotherm $H$ is sufficiently larger than that of the dilating center $D$, the magnetic potential can be represented by eqs. (53), yielding the magnetic field;

$$
\left.
\begin{aligned}
\frac{X_H}{C_H}&=-\frac{3\lambda+4\mu}{2(\lambda+\mu)}\left(\frac{1}{\rho_1^3}-\frac{3x^2}{\rho_1^5}\right) \\
\frac{Y_H}{C_H}&=\frac{3(3\lambda+4\mu)}{2(\lambda+\mu)}\frac{xy}{\rho_1^5} \\
\frac{Z_H}{C_H}&=-\frac{3(3\lambda+4\mu)}{2(\lambda+\mu)}\frac{xD_1}{\rho_1^5} \\
\frac{X_V}{C_V}&=\frac{3(3\lambda+2\mu)}{2(\lambda+\mu)}\frac{xD_1}{\rho_1^5} \\
\frac{Y_V}{C_V}&=\frac{3(3\lambda+2\mu)}{2(\lambda+\mu)}\frac{yD_1}{\rho_1^5} \\
\frac{Z_V}{C_V}&=\frac{3\lambda+2\mu}{2(\lambda+\mu)}\left(\frac{1}{\rho_1^3}-\frac{3D_1^2}{\rho_1^5}\right)
\end{aligned}
\right\} \tag{55}
$$

## Discussion and Concluding Remarks

We will investigate some general characteristics of the piezomagnetic field accompanying the Mogi model. Let us first examine what amount of magnetic changes we may expect in this model. According to eqs. (50) and (54), the magnetic field intensity is proportional to

$$C_S = 2\pi\beta J_0 \frac{C}{D^3} = \pi\beta J_0 \left(\frac{a}{D}\right)^3 \Delta P \tag{56}$$

We tentatively assume numerical values employed by DAVIS (1976) for the Kilauea volcano, *i.e.*, $\beta = 2\times10^{-4}\,\mathrm{bar}^{-1}$, $J_0 = 5.0\times10^{-3}$ emu/cc, $a/D = 1/4$ and $\Delta P = 3$ kbars, which give rise to $C_S = 1.47\times10^{-4}$ Oe $= 14.7\,\gamma$. Such a high internal pressure as 3 kbars is estimated by DAVIS (1976) to interpret the surface tilt of up to $10^{-4}$ observed at the time of the 1971 eruptions.

There might yet be room for yielding greater piezomagnetic effect by assuming larger values of $J_0$ and/or $\beta$. The factor $C_S$ is, however, highly dependent on the ratio $a/D$ and the internal pressure $\Delta P$. These values are constrained by the mechanical strength of chamber wall rocks, which must bear stresses typically represented by eq. (9). A conventional way of avoiding the unreasonably high pressure which is often adopted is to presume the overall rigidity of volcanic body to be much smaller than that of ordinary rocks, which directly results in an order of magnitude reduction of the $C_S$ value. It might be difficult to expect stress-induced volcanomagnetic changes exceeding 10 gammas, in so far as ordinary values are assumed for the internal pressure within the volcano to be, at most, several thousand bars.

In the next place, we will investigate the influence of $H$, the depth of Currie point isotherm. In Fig. 3 are shown $X_H$ and $Z_V$ components at the coordinate origin (0, 0, 0), the surface point just above the dilating center, as functions of $H$. This figure tells us:

(1) When $H$ is small compared with $D$, the magnetic field at the surface is comparatively small. In both $X_H$ and $Z_V$ component, a minor minimum stage appears at a shallow depth.

(2) Immediately after $H$ passes the depth of the dilating center, the magnetic field abruptly begins to decrease, approaching rapidly the asymptotic values at $H$ infinity. The extreme values give the maximum absolue field changes and are attained nearly at a depth of $H\sim2D$. The main contributor to the surface field is the stress-induced magnetization within a layer $D\leqq z'\leqq 2D$. The present result comes from the fact: the shearing stress of the center of dilatation in the upper region $(0<z'<D)$ cancels the magnetic field produced by normal stresses, while that in the lower region augments them.

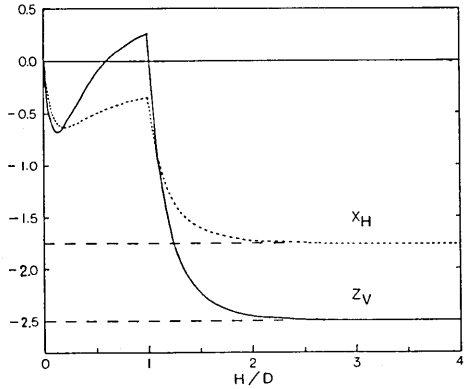


Fig. 3. $X_H$ and $Z_V$ components at the surface point just above the dilating center as functions of the Currie depth $H$.

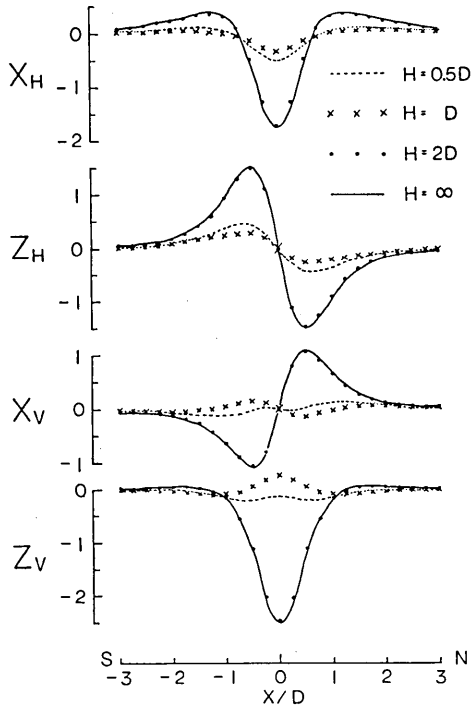


Fig. 4. $X_H$, $Z_H$, $X_V$ and $Z_V$ components along the $x$ axis in unit of $C_S$, for some typical values of the Currie depth $H$.

A similar figure was illustrated for the $Z_V$ component by DAVIS (1976), who conducted numerical integrations. His result (Fig. 2(a) in his paper) is, however, quite different from the present one. He showed that $Z_V$ increases until $H$ arrives at $D$, and that it then decreases to a certain value. The maximum absolute field change is attained when $H=D$, in contrast to the present result that it is obtained when $H=\infty$. Since details are not given on the numerical

calculation procedure in Davis' paper, the writer cannot understand exactly the reason why such a discrepany is brought about.

Fig. 3 shows that an extreme case solution (55) should be a good approximation of the rigorous one (54) when $H>2D$. This will be clearly demonstrated in Fig. 4, where $X_H$, $Z_H$, $X_V$ and $Z_V$ components along the $x$ axis are illustrated for some different values of $H$. The curves for the case $H=2D$ almost coincide with those for $H=\infty$. The magma chamber has usually been presumed to be located at a shallower depth, a few km say, while the Currie depth is not so different from ordinary crust, about 20 km or so. The solution (55) seems therefore to hold good in almost all cases in considering the stress-induced volcanomagnetic effect.

A comparison will be made qualitatively between two possible causes of the volcanomagnetic effect; (a) stress-induced magnetization, and (b) thermal demagnetization and re-magnetization of volcanic rocks. The latter case is simply modelled here by changes in the uniform magnetization $\Delta J=J_0(T_2)-J_0(T_1)$ in a sphere of radius $a$ placed at $(0, 0, D)$. The magnetic potential for the "stress effect" model is given by ($\lambda=\mu$ is assumed)

$$W_S=\frac{7}{4}C_S\cos I_0\frac{xD^3}{\rho_1^3}+\frac{5}{4}C_S\sin I_0\frac{(D-z)D^3}{\rho_1^3} \tag{57}$$

and for the "temperature effect" model by

$$W_T=-C_T\cos I_0\frac{xD^3}{\rho_1^3}+C_T\sin I_0\frac{(D-z)D^3}{\rho_1^3} \tag{58}$$

where

$$C_T=\frac{4\pi}{3}\left(\frac{a}{D}\right)^3\Delta J_0 \tag{59}$$

and $I_0$ denotes the magnetic dip of the magnetization parallel to the ambient geomagnetic field.

Remarkable magnetic changes were observed on the Oshima volcano at the time of 1950 great eruption (RIKITAKE 1951), the 1953-54 moderate activities (YOKOYAMA 1956) and the 1957 minor eruption (YUKUTAKE and YABU 1962). Geomagnetic changes were attributed to the temperature variation within the volcano by these authors. We now compare, as an example, magnetic changes by the stress and thermal origin for the case of the Oshima volcano.

We tentatively put (a) $a/D=1/4$, $J_0=5.0\times10^{-2}$emu/cc, $\beta=1.0\times10^{-4}$ bar$^{-1}$ and $\Delta P=500$ bars, which yield $C_S=12.3\ \gamma$, and (b) $a/D=1/4$, $\Delta J_0=1.0\times10^{-2}$ emu/cc, which give rise to $C_T=65.4\ \gamma$. The stress sensitivity

$\beta$ of lavas from the Oshima volcano was actually measured by OHNAKA and KINOSHITA (1968). The latter magnetization change $\Delta J_0$ is presumed by YOKOYAMA (1969) to correspond to the temperature change from 150°C to 200°C for typical rock samples. This shows that the conventional temperature effect could produce magnetic changes very effectively, except for an alternative difficulty of finding the rapidly heating and cooling mechanism of the volcanic body (UYEDA 1961).

Figs. 5(a), (b), (c) and (d) show the $H$, $D$, $Z$ and $F$ component variations caused by the stress and temperature effect respectively, to be observed at the surface around the Oshima volcano. $I_0$ is taken here 47° 50′. These variation patterns imply the deviation from its normal state to (a) the stressed and (b) hot state respectively. Fig. 5(b) shows that both models result in a westward increase of the declination on the western side of the volcano at the inflated and hot stage respectively. It is the best established observational fact at the Nomashi Observatory (about 3 km west of the summit crater) that the $D$ component varies westward before eruptions. The long-period changes in the declination at Nomashi was sufficiently interpreted by YOKOYAMA (1969), who proposed a cooling mechanism by rainfalls into the summit caldera. The piezomagnetic change might be responsible for the rapid eastward recovery of the $D$ component at Nomashi soon after the 1953-54 eruptions.

The $F$ component variations for both models are characterized by a strong but rather localized decrease. The maximum decrease is

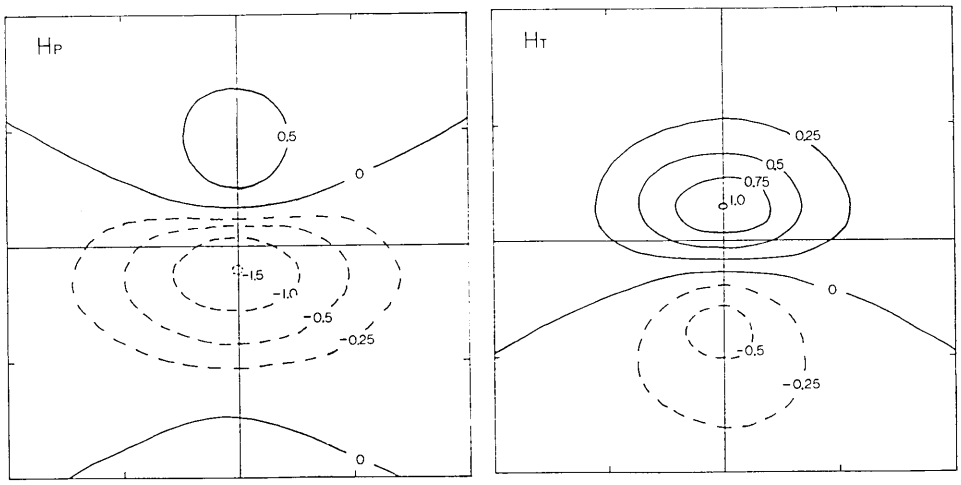


Fig. 5(a). Magnetic north component on the surface due to the stress effect in unit of $C_S$ (on the left hand side) and the temperature effect in unit of $C_T$ (on the right hand side) respectively. The magnetic dip $I_0$ is taken to be 47°50′, which is the average value around the Oshima volcano.

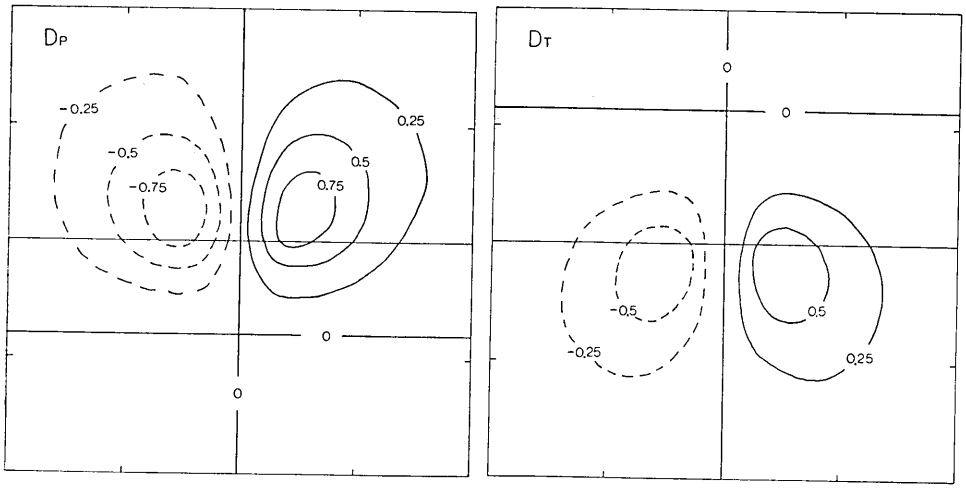


Fig. 5(b). Magnetic east component due to the stress (left) and temperature effect (right) respectively.

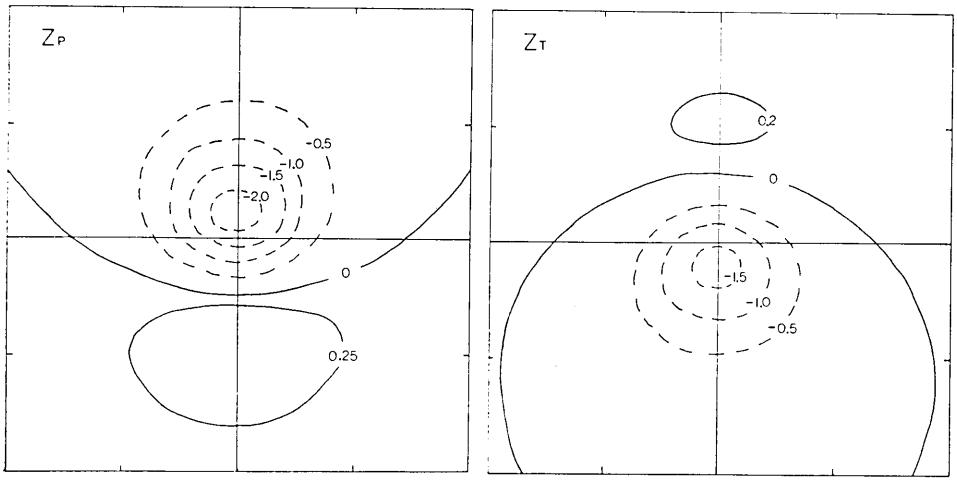


Fig. 5(c). Magnetic vertical component with positive downward due to the stress (left) and temperature effect (right) respectively.

expected to occur just upon the crater in case of the stress effect model. This might bring about some obstacles in practically monitoring the volcanic activity by the magnetic method. All these figures might provide us some useful suggestions for the optimum arrangement of observation points.

Parameters yielding the $C_S$ value for the case of the Oshima volcano are estimated rather too large, while moderate values are adopted for $C_T$. Hence the stress-induced volcanomagnetic effect, if it does

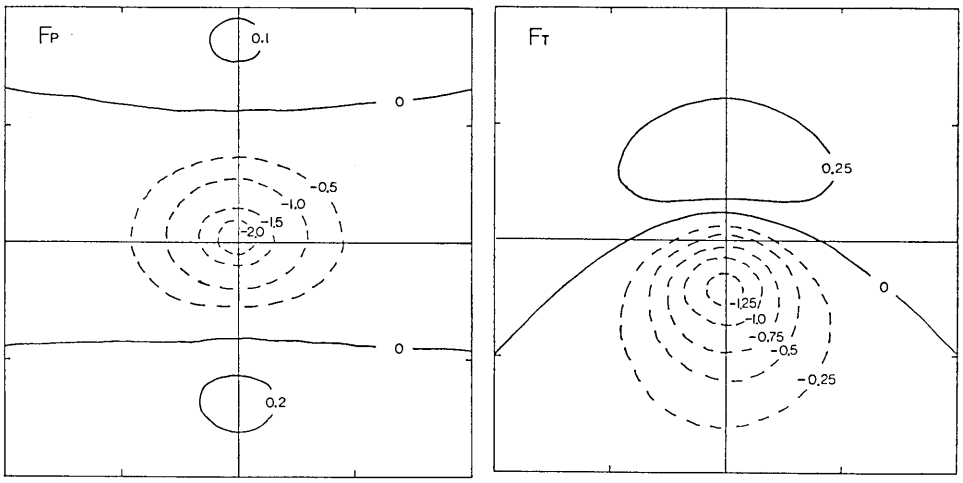


Fig. 5(d). Magnetic total force intensity due to the stress (left) and temperature effect (right) respectively.

exist, might be a secondary one even in the case of the Oshima volcano. Both models are compatible at the active stage of a volcano, although the time-dependent behavior might be different. If we take into account some suitable combinations of the two effects, possibly together with the idea of a moving source as proposed by UYEDA (1961), we may be able to arrive at a more comprehensive understanding of the observed volcanomagnetic effect on the Oshima volcano.

According to eq. (57), a considerable positive change in the $F$ component is expected for Kilauea at the time of stress discharge due to eruptions, as far as we employ the numerical value of $C_S$ adopted by DAVIS (1976). No appreciable geomagnetic changes were, however, observed at the time of 1971 eruption (DAVIS *et al.* 1973). The important conclusion of DAVIS (1976), seemingly valid for the Kilauea volcano, is that a more effective mechanism than a simple Mogi model is necessary for interpreting the observed surface deformations and geomagnetic changes consistently.

There still remain some problems unsolved with respect to the magnetic changes accompanying the Mogi model. In his solution of the gravity change associated with the Mogi model, HAGIWARA (1977) discriminates four types of contributions to the gravity change. They are (1) free-air gravity change accompanying the ground uplift, (2) Bouguer change caused by the excess mass corresponding to the upheaved portion of the free surface, (3) the effect of the loss of surrounding mass by the expanding force source, and (4) the gravity change

produced by density changes within the semi-infinite earth. Similarly four ways of generating the magnetic change are conceivable. The piezomagnetic field considered so far is nothing but the type (4) change.

The first type effect, the magnetic change that may be caused by the ground uplift, is negligibly small, because the geomagnetic dipole moment is comparatively weak. At middle latitudes, such as in Japan the vertical gradients of the main geomagnetic field are $\partial H_0/\partial z \sim -0.015\,\gamma/m$, and $\partial Z_0/\partial z \sim -0.018\,\gamma/m$. The third effect can also be ignored since the volumetric change in the source sphere is very little.

The second type effect of the surface deformation, or the displacements of the magnetized body near the observation point, might produce observable magnetic changes. For example, MORI *et al.* (1978) successfully explained magnetic changes observed around the volcano Usu, in Hokkaido, Japan, at the time of the 1977 activity with special reference to its dome-forming movements. It is not an easy matter, however, to estimate the magnetic field from the deformed portion of the magnetized body in a general way, although RIKITAKE (1951)'s work on the magnetic field over a circular cone may be very helpful to the present problem. Possible magnetic changes caused by the surface displacements remain as a future subject.

## Acknowledgements

The writer greatly acknowledges professor Y. Hagiwara, for his impetus to the present work and constant advice in the course of the study. Sincere thanks are also due to associate professor T. Maruyama, who kindly gave useful suggestions on some aspects of Fourier transforms. Thanks also to professor T. Yukutake for critically reading the manuscript and giving valuable comments.

## Appendix Derivation of Fourier transforms in Table 1.

Let us first consider the Fourier transform of a simple function $f_1(x, y)=1/\sqrt{x^2+y^2+\zeta^2}$ $(\zeta>0)$, *i.e.*

$$f_1^*(\xi, \eta)=\frac{1}{2\pi}\iint_{-\infty}^{\infty}\frac{1}{\sqrt{x^2+y^2+\zeta^2}}\,e^{-i(\xi x+\eta y)}dxdy \tag{A1}$$

Substituting

$$x=r\cos\theta,\ y=r\sin\theta,\ \xi=\alpha\cos\varphi,\ \eta=\alpha\sin\varphi \tag{A2}$$

eq. (A1) reduces to

$$f_1^*(\xi, \eta)=\int_0^\infty \frac{1}{\sqrt{r^2+\zeta^2}} J_0(\alpha r) r dr \tag{A3}$$

which makes use of Hansen's integral representation of Bessel function $J_n(\alpha r)$:

$$J_n(\alpha r)=\frac{(-1)^n}{2\pi}\int_0^{2\pi} e^{i\alpha r \cos \varphi} \cos n\varphi d\varphi \tag{A4}$$

Multiplying eq. (A4) for $n=0$ by $e^{-\alpha\zeta}$ and integrating it with respect to $\alpha$, we can evaluate the following integral (WATSON, 1922),

$$\int_0^\infty e^{-\alpha\zeta} J_0(\alpha r) d\alpha=\frac{1}{\sqrt{r^2+\zeta^2}} \quad (\zeta>0) \tag{A5}$$

Hankel's inversion theorem is then applied to eq. (A5) and we obtain

$$\frac{1}{2\pi}\iint_{-\infty}^{\infty} \frac{1}{\sqrt{x^2+y^2+\zeta^2}} e^{-i(\xi x+\eta y)} dxdy=\int_0^\infty \frac{1}{\sqrt{r^2+\zeta^2}} J_0(\alpha r) r dr=\frac{e^{-\alpha\zeta}}{\alpha} \tag{A6}$$

Differentiating this equation with respect to $\zeta$, we have the following formula;

$$\frac{1}{2\pi}\iint_{-\infty}^{\infty} \frac{1}{(x^2+y^2+\zeta^2)^{3/2}} e^{-i(\xi x+\eta y)} dxdy=\frac{e^{-\alpha\zeta}}{\zeta} \tag{A7}$$

which is equivalent to (F1) in Table 1. If we take derivatives of both sides of eq. (A7) with respect to $\xi$, $\eta$ or $\zeta$, we may find Fourier transform formula (F2) to (F9) in Table 1.

We are now to consider the Fourier transform

$$f_2^*(\xi, \eta)=\frac{1}{2\pi}\iint_{-\infty}^{\infty} \frac{x^2}{x^2+y^2} \frac{1}{(x^2+y^2+\zeta^2)^{3/2}} e^{-i(\xi x+\eta y)} dxdy \tag{A8}$$

By making use of relations (A2) and (A4), eq. (A8) becomes

$$f_2^*(\xi, \eta)=\frac{1}{2}\int_0^\infty \frac{1}{\rho^3}\left\{ r J_0(\alpha r)-\frac{\xi^2-\eta^2}{\alpha^2} r J_2(\alpha r) \right\} dr \tag{A9}$$

With the aid of the recurrence formulae of Bessel functions, we obtain

$$f_2^*(\xi, \eta)=-\frac{\xi^2-\eta^2}{\alpha^4}\frac{1}{\zeta^3}+\frac{\xi^2}{\alpha^2}\int_0^\infty \frac{1}{\rho^3} J_0(\alpha r) r dr+3\frac{\xi^2-\eta^2}{\alpha^4}\int_0^\infty \frac{1}{\rho^5} J_0(\alpha r) r dr \tag{A10}$$

Integrals on the right hand side are Fourier transforms of $\rho^{-3}$ and $\rho^{-5}$ respectively, which are already known in Table 1. The Fourier transform of $f_2(x, y)$ is thus obtained as

$$f_2^*(\xi, \eta)=\frac{\eta^2-\xi^2}{\alpha^4}\frac{1}{\zeta^3}+\left(\frac{\xi^2}{\alpha^2}\cdot\frac{1}{\zeta}+\frac{\xi^2-\eta^2}{\alpha^3}\cdot\frac{1}{\zeta^2}+\frac{\xi^2-\eta^2}{\alpha^4}\cdot\frac{1}{\zeta^3}\right)e^{-\alpha\zeta} \tag{A11}$$

which is equivalent to the formula (F10) in Table 1. The formulae (F11) and (F12) will be given by taking derivatives of (A11) with respect to $\zeta$.

We can derive the formula (F13) in a similar way as described above. The differentiation of (F13) leads us to eqs. (F14) and (F15).

## References


ANDERSON, E. M., 1936, The dynamics of the formation of cone-sheets, ring-dykes and cauldron subsidences, *Proc. Roy. Soc. Edin.*, **56**, 128-157.

DAVIS, P. M., 1976, The computed piezomagnetic anomaly field for Kilauea Volcano, Hawaii, *J. Geomag. Geoelectr.*, **28**, 113-122.

DAVIS, P. M., D. B. JACKSON, J. FIELD and F. D. STACEY, 1973, Kilauea volcano, Hawaii: A search for the volcanomagnetic effect, *Science*, **180**, 73-74.

FISKE, R. S. and W. T. KINOSHITA, 1969, Inflation of Kilauea Volcano prior to its 1967-1968 eruption, *Science*, **165**, 341-349.

HAGIWARA, Y., 1977, The Mogi model as a possible cause of the crustal uplift in the eastern part of Izu Peninsula and related gravity change (in Japanese), *Bull. Earthq. Res. Inst.*, **52**, 301-309.

MINDLIN, R. D. and D. H. CHENG, 1950, Nuclei of strain in the semi-infinite solid, *J. Applied Phys.*, **21**, 926-930.

MOGI, K., 1958, Relations between the eruptions of various volcanoes and the deformations of the ground surfaces around them, *Bull. Earthq. Res. Inst.*, **36**, 99-134.

MORI, T., A. OOCHI, K. HASEGAWA, Y. SASAI, M. SAWADA and Y. NISHIDA, 1978, Geomagnetic and telluric current observation around the Usu volcano (in Japanese), in *Proceedings of the Conductivity Anomaly Symposium, CA Group Japan.*

NAGATA, T., 1970, Basic Magnetic properties of rocks under the effects of mechanical stresses, *Tectonophysics*, **9**, 167-195.

OHNAKA, M. and H. KINOSHITA, 1968, Effects of uniaxial compression on remanent magnetization, *J. Geomag. Geoelectr.*, **20**, 93-99.

RIKITAKE, T., 1951, The distribution of magnetic dip in Ooshima (Oosima) Island and its change that accompanied the eruption of Volcano Mihara, 1950, *Bull. Earthq. Res. Inst.*, **24**, 161-181.

STACEY, F. D., K. G. BARR and G. R. ROBSON, 1965, The volcanomagnetic effect, *Pure Appl. Geophys.*, **62**, 96-104.

STACEY, F. D. and S. K. BANERJEE, 1974, *The Physical Principles of Rock Magnetism. Ch.* 11 *Piezomagnetic Effects*, Elsevier.

UYEDA, S., 1961, An interpretation of the transient geomagnetic variations accompanying the volcanic activities at Volcano Mihara. Oshima Island, Japan, *Bull. Earthq. Res. Inst.*, **39**, 579-591.

WATSON, G. N., 1922, *A treatise on the theory of Bessel functions*, 4th ed., Cambridge.

YAMAKAWA, N., 1955, On the strain produced in a semi-infinite elastic solid by an interior source of stress (in Japanese), *J. Seismol. Soc. Japan*, (ii) **8**, 84-98.

YOKOYAMA, I., 1956, Geomagnetic studies of Volcano Mihara, the 7th paper, *Bull. Earthq. Res. Inst.*, **34**, 21-32.

YOKOYAMA, I., 1969, Anomalous changes in geomagnetic field on Ooshima Volcano related with its activities in the decade of 1950, *J. Phys. Earth*, **17**, 69-76.

YOKOYAMA, I., 1971, A model for the crustal deformation around volcanoes, *J. Phys. Earth*, **19**, 199-207.

YUKUTAKE, T. and T. YABU, 1962, Geomagnetic studies on Volcano Mihara, the 9th paper, *Bull. Earthq. Res. Inst.*, **40**, 511-522.

YUKUTAKE T. and H. TACHINAKA, 1967, Geomagnetic variation associated with stress change within a semi-infinite elastic earth caused by a cylindrical force source, *Bull. Earthq. Res. Inst.*, **45**, 785-798.

---

## 1. 茂木モデルに伴うピエゾ磁気変化

地震研究所　笹井洋一

茂木 (1958) は火山噴火に伴う地殻変動を理解するモデルとして，半無限弾性体中に置かれた一様膨張の点力源による地表の変形を考えた．この茂木モデルに伴う応力によって，地殻の帯磁が変化する（可逆的ピエゾ磁気効果）ので，それによる磁場変化を求めた．地表面から地殻のある深さまで一様帯磁していると仮定し，力源の大きさを無視すると，地上での磁場変化の解が解析的に得られる．この解は，地下の幾つかの点に置かれた磁気双極子と四重極の組合せより成る．特にキュリー点等温面が力源より十分深いならば，地上での磁場は力源の位置に置かれた双極子によるそれでよく近似できる．

伊豆大島三原山の西にある野増の地磁気観測所では，噴火に先立って偏角が西偏し，噴火の後に東偏する例が知られている．この変化は従来，火山体の熱消磁で説明されてきたが，応力変化でも同様な現象が生じ得ることが分った．野増における偏角変化の少なくとも一部は，ピエゾ磁気効果で説明できるかもしれない．

---